Supplementary Information for:

Summertime State-Level Source-Receptor Relationships between NO_x Emissions and Downwind Surface Ozone Concentrations over the Continental United States

Daniel Q. Tong (tong.daniel@epa.gov)[1,2,3]

and

Denise L. Mauzerall (mauzeral@princeton.edu)[1,4,5]

11 pages, five Figures and one Table.

S1. CMAQ Model Configuration

CMAQ is configured with detailed implementation of horizontal and vertical advection based on the Piecewise Parabolic Method (PPM), turbulent diffusion based on K-theory, chemistry in the gas, liquid, and particulate phases using a modified version of the CBM-IV chemical mechanism (CB4-AQ-AE3) (*Gery et al., 1994*), dry deposition, and cloud physics and chemistry (CLOUD-RADM) (*15*). Hourly meteorological parameters, including temperature, wind velocities, humidity, surface pressure, and solar radiation, are obtained from the 5th Generation Mesoscale Model (MM5) (*Grell et al., 1994*). Anthropogenic emissions of nitrogen oxides (NO_x), sulfur dioxide (SO_2), carbon monoxide (CO), volatile organic compounds (VOCs), and ammonia (NH_3) are obtained from the county level U.S. EPA 1996 National Emissions Trends inventory and processed with the Sparse Matrix Operator Kernel Emissions (SMOKE) model (*Houyoux et al., 2000*). Vehicle emissions of NO_x, VOCs, CO and primary particulate matter (PM) are prepared using MOBILE5 (*US EPA, 2003*). Biogenic emissions, including NO_x and VOCs, are obtained from the biogenic emissions inventory system, version 3 (BEIS3) (*Pierce et al., 1998*).

We chose 1996 emissions and meteorology because we have already carefully evaluated model results with observations using this data (*16*). Figure S1 shows the monthly mean surface wind in July 1996 over the continental U.S. obtained from the MM5 simulation which provides the meteorological fields for our CMAQ simulation. Ideally current emission data and meteorology would be used for analysis, particularly for NO_x for which increasingly stringent controls on large stationary sources have been implemented over the last decade (*23*). However, at the time this work was started, even the 2002 National Emission Inventory (NEI), which did not fully account for the OTC emission reduction program, was not yet available.

S2. Biogenic NO_x Emissions

Figure S2 shows the spatial distribution of isoprene and NO_x emissions over our model domain. The figures show that while biogenic isoprene emissions are mostly

emitted from forested areas, biogenic NO_x is emitted predominantly from agricultural lands. Over rural areas, soil-biogenic NO_x emissions dominate other sources. Due to the human influence on emissions of soil-biogenic NO_x via nitrogenous fertilizer application, we remove biogenic as well as direct anthropogenic emissions of NO_x from our perturbation simulations in order to quantify the total effect a source state's NO_x emissions have on intra- and inter-state O_3 concentrations.

Unlike biogenic VOCs such as isoprene, trees are not a significant contributor to biogenic NO_x emissions in regions other than tropical forests. Yienger and Levy (*1995*) estimated that forests only contribute 1 – 2% of total biogenic NO_x emissions in temperature regions. Previous field measurements in the U.S. revealed that forest emissions are one order of magnitude lower than those of grassland, which is about one tenth that of heavily fertilized soils (*Williams and Fehsenfeld, 1991*).

S3. Model Evaluation

Prior to using CMAQ to quantify source-receptor relationships we evaluated the ability of the model to simulate the surface distribution of tropospheric O_3 (*16*). A map of the model domain and measurement sites is shown in Figure S3. CMAQ reproduces surface O_3 for a wide range of conditions (30-80 ppbv) with a normalized mean error (NME) less than 35% and normalized mean bias (NMB) lying between ±15% for the whole domain. The NME is the averaged magnitude of the difference between model prediction and observation normalized by the observation. The NMB is defined similarly, but considers the actual difference, instead of the absolute value, allowing over- and under-estimation to cancel out. Although systematically over-predicting O_3 in the eastern US and coastal locations and under-predicting it in the California Central Valley and many locations in the western US, the model is able to reproduce 1-hour and 8-hour daily maxima with a cross-domain mean bias (MB) of 1 ppbv and 8 ppbv, or NMB of 8% and 25%, respectively.

Comparisons of vertical profiles of simulated O_3 with ozonesonde data show a consistent under-prediction in the upper troposphere even when lateral boundary conditions from MOZART-2 are used (*16*). The discrepancy can be attributed to the use of a zero-flux upper boundary condition in CMAQ with a relatively low model top

(200mb) (*16*). In addition, missing sources of NO_x emissions, such as transported NO_x from the stratosphere, lightning and aircraft discharges, may play an important role in determining O_3 concentrations in the upper troposphere. Lightning accounts for roughly 14% of NO_x emissions in July over the continental U.S., and its emissions have been shown to contribute a significant fraction to O_3 concentrations in the middle and upper troposphere (*Zhang et al., 2003 and references therein*). Aircraft emissions increase background NO_x concentrations by 0.05-0.07 ppbv in the upper troposphere over North America, and contribute up to 3 ppbv to upper troposphere O_3 levels in July (*Kentarchos et al., 2002*). Although air traffic related emissions near the surface are included in the model input, aircraft emissions at high altitudes are not. The under-prediction of O_3 at high altitudes may raise questions about the ability of CMAQ to simulate continental scale pollution transport. Long-distance transport of air pollution at mid-latitudes is generally associated with lifting of surface emissions to the free troposphere by frontal systems or convection followed by rapid advection in the free troposphere westerlies and subsidence at downwind locations (*Bey et al., 2001; Cooper et al., 2003).* O_3 is the primary precursor of the hydroxyl radical which in turn determines the lifetime of most atmospheric constituents. Therefore, the underestimation of upper tropospheric O_3 concentrations may change the lifetime of O_3 and its precursors in the upper troposphere and thus change the distance of transport and the source-receptor relationships. However, as the major objective of this study is to examine the impact of large NO_x emissions on downwind surface locations, the long-distance transport processes in the upper troposphere are less important than advection and photochemistry near the surface. *Mauzerall et al*. (*1996*) has shown that photochemistry largely controls O_3 concentrations in the polluted boundary layer. We expect the underestimation of upper tropospheric O_3 due to exclusion of the influx of stratospheric O_3 to have only a small effect on our results.

S4. Spatial distribution of surface O_3 in source and receptor states

Figure S4 shows the spatial distribution of changes in mean July all-hour O_3 concentrations resulting from NO_x emissions from ten states distributed across the U.S.

These states include the five largest NO_x emitters (TX, CA, OH, IL, and FL), two ranked in the top 25% (PA and TN), and three with moderate emissions (NY, NJ and CO).

S5. Time Series of Hourly O_3 Concentrations over Trenton, NJ

To illustrate the different sensitivities between peak 8-hour and 24-hour O_3 concentrations to NO_x emission changes, we provide a time series showing hourly O_3 concentrations with and without New Jersey NO_x emissions over Trenton, NJ. Figure S5 shows that most days local NO_x emissions reduce surface O_3 concentrations at night and in early morning but increase peak O_3 concentrations during the day. Although the relative magnitude of increases or decreases caused by local emissions vary spatially and depend upon meteorological conditions, the general trends with and without intrastate emissions are similar. As a result, the state-averaged 24-hour and peak 8-hour metrics display different responses to NO_x emission changes.

References:

Bey, I., D.J. Jacob, J.A. Login, and R.M. Yantosca. Asian chemical outflow to the Pacific: Orgins, pathways and budgets, *J. Geophys. Res.*, **2001,** 106, 23,097 – 23,114.

Cooper, O.R., J.L. Moody, D.D. Parrish, M. Trainer, T.B. Ryerson, J.S. Holloway, G. Hubler, F.C. Fehsenfeld, and M.J. Evans. Trace gas composition of midatlantic cyclones over the western North Atlantic Ocean: A conceptual mode, *J. Geophys. Res.*, 107(D7), **2002,** 4056, doi:10.1029/2001JD000901.

Gery, M. W.; Whitten, G. Z.; Killus, J. P.; Dodge, M. C., A photochemical kinetic mechanism for urban and regional scale computer modeling. *J. Geophys. Res.* **1994,** *94*, 12,925-12,956.

Grell, G. A.; Dudhia, J.; Stauffer, D. R., A description of the Fifth-Generation Penn State/NCAR Mesoscale Model (MM5). *NCAR Technical Note* **1994**.

Houyoux, M. R.; Vukovich, J. M.; Coats Jr., C. J.; Wheeler, N. J. M.; Kasibhatla, P. S., Emission inventory development and processing for the Seasonal Model for Regional Air Quality (SMRAQ) project. *J. Geophys. Res.* **2000,** *105*, (D7), 9079–9090.

Kentarchos A. S., and G. J. Roelofs. Impact of aircraft NO x emissions on tropospheric ozone calculated with a chemistry-general circulation model: Sensitivity to higher hydrocarbon chemistry, J. Geophys. Res., **2002**,107 (D13), 4175, doi:10.1029/2001JD000828.

Mauzerall, D. L., Jacob, D. J., Fan, S. M., Bradshaw, J. D., Gregory, G. L., Sachse, G. W. and Blake, D. R., "Origin of Tropospheric Ozone at Remote High Northern Latitudes in Summer," *J. Geophys. Res.*, 101, pp. 4175-4188, 1996.

Parrish, D.D. Critical evaluation of US on-road vehicle emission inventories. *Atmospheric Environment*, **2006,** *40(13)*, *2288-2300.*

Pierce, T.; Geron, C.; Bender, L.; Dennis, R.; Tonnesen, G.; Guenther, A., Influence of increased isoprene emissions on regional ozone modeling. *J. Geophys. Res.* **1998,** *103*, (D19), 25,611–25,629.

U.S. Environmental Protection Agency (US EPA), 2003. User's guide to MOBILE6.1 and MOBILE6.2. Office of Air and Radiation, EPA420-R-03-010, Assessment and Standards Division, Office of Transportation and Air Quality, U.S. Environmental Protection Agency.

Williams, E.J.; Fehsenfeld, F.C. Measurement of soil nitrogen oxides emissions at three North American ecosystems, *J. Geophys. Res.* **1991**, 96, 1033-1042.

Yienger, J.J; Levy, H. Empirical model of global soil-biogenic NO_x emissions. *J. Geophys. Res.* **2003**, 100(D6), 11,447.

Zhang R.Y, X.X. Tie, and D.W. Bond. Impacts of anthropogenic and natural NOx sources over the U.S. on troposphere chemistry, *Proceedings of National Academic Sciences,* **2003**, 100(4), page 1505-1509.

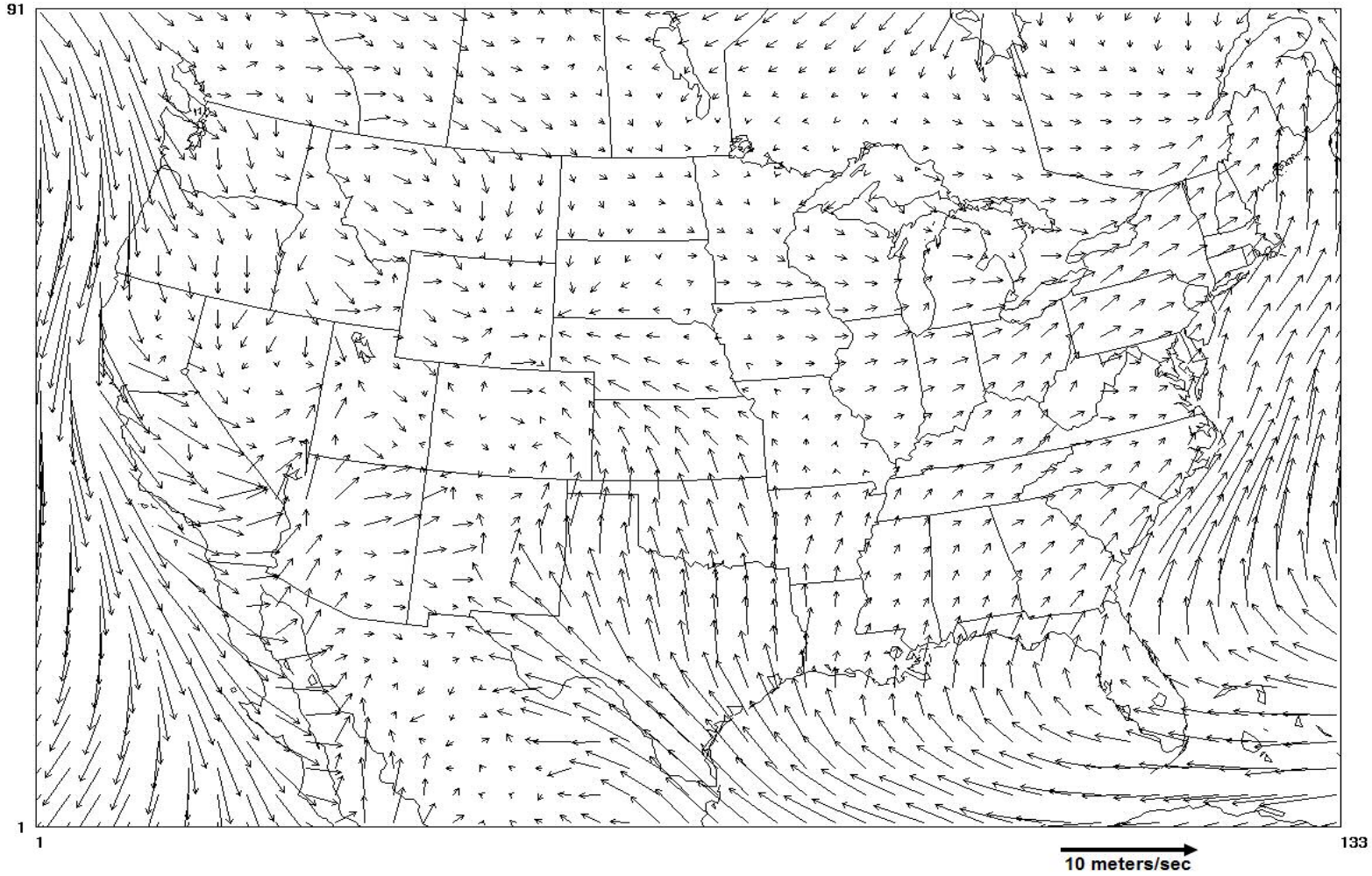

Figure S1. Monthly mean surface winds in July 1996 over the continental United States. Winds are from the MM5 simulation that provides the meteorological fields used for CMAQ.

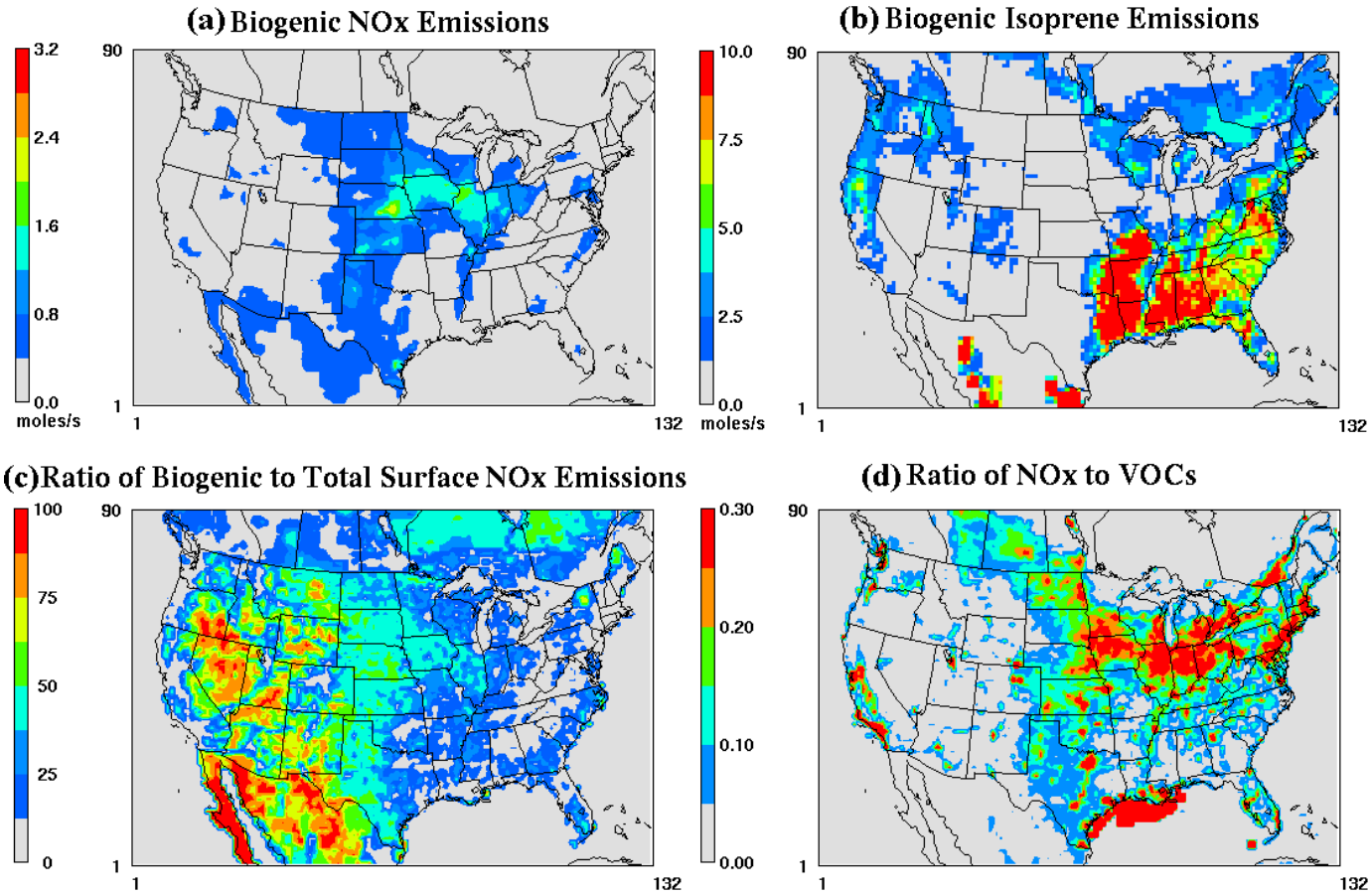

Figure S2. Spatial distribution of mean July 1996 a) biogenic NO_x emissions, b) biogenic isoprene emissions, c) the ratio of biogenic NO_x emissions to total surface NO_x emissions and d) the ratio of NO_x emissions to total VOC emissions over our domain.

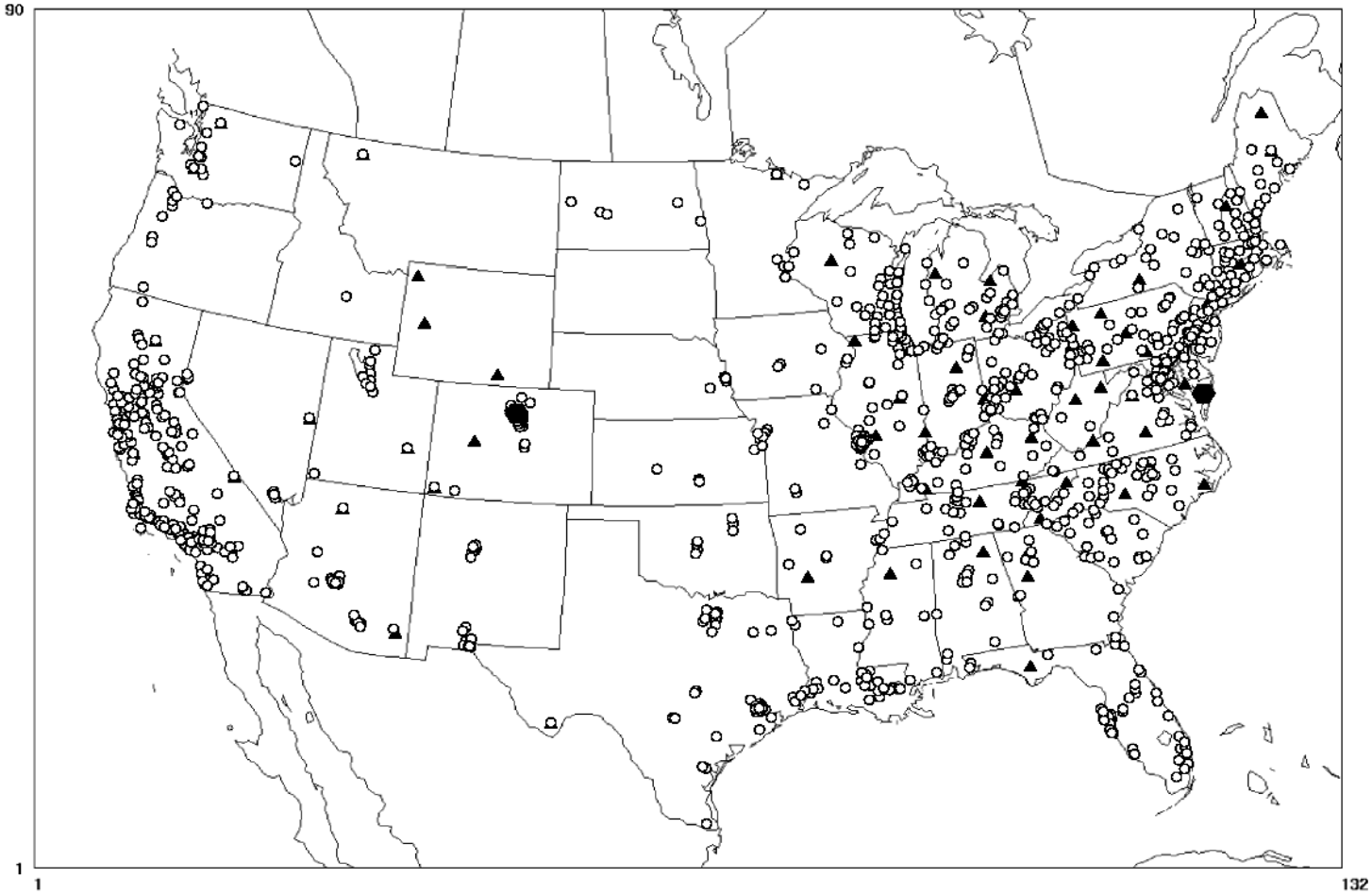

Figure S3. Map of modeling domain and locations of measurements used for model evaluation. Open circles are AQS monitors, filled triangles are CASTNet sites, and filled circles are two ozonesonde stations located at Boulder, CO and Wallops Island, VA.

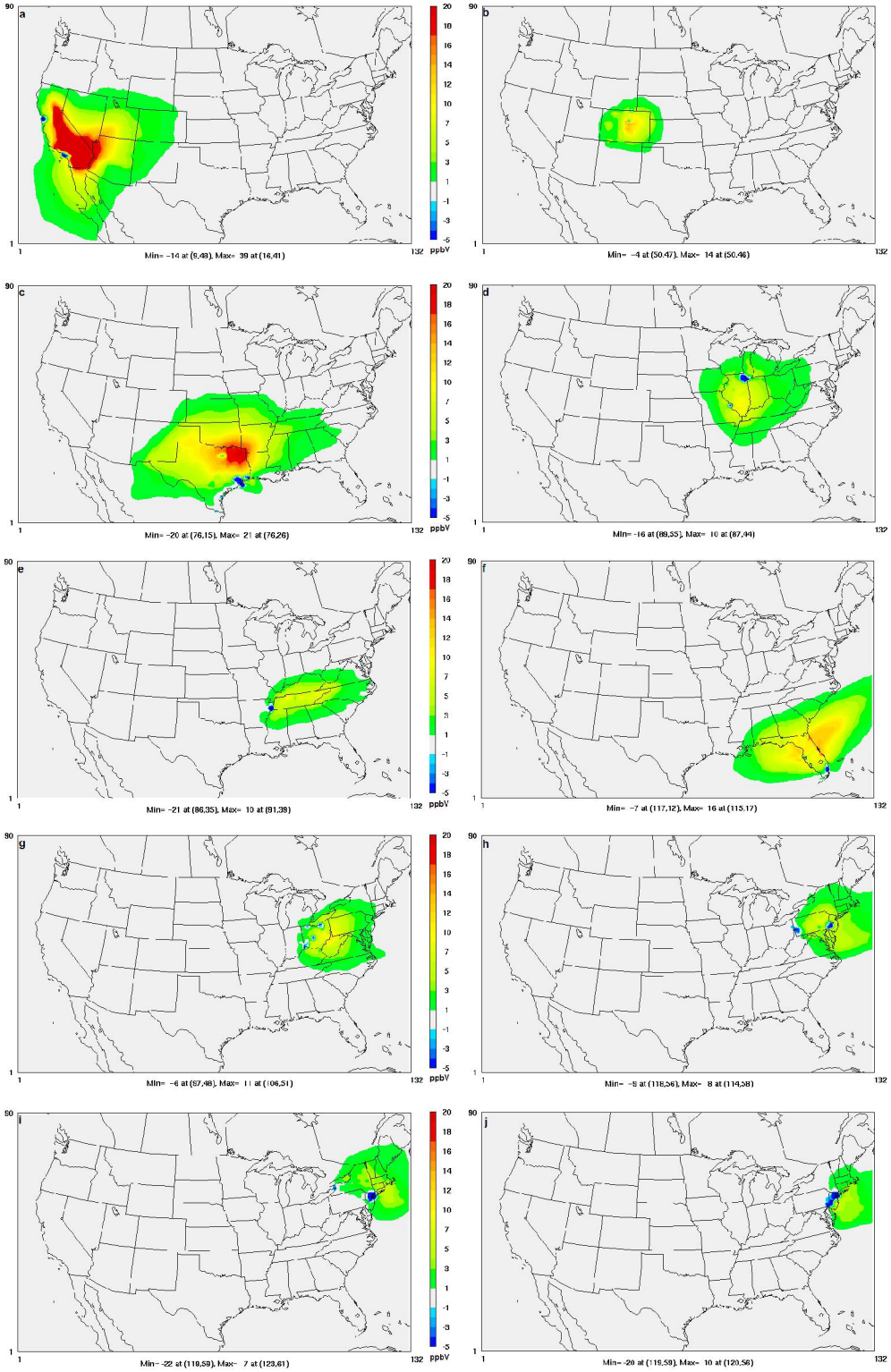

Figure S4. Changes in monthly mean all-hour O_3 concentrations resulting from NO_x emissions from: (a) California; (b) Colorado; (c) Texas; (d) Illinois; (e) Tennessee; (f) Florida; (g) Ohio; (h) Pennsylvania; (i) New York and (j) New Jersey.

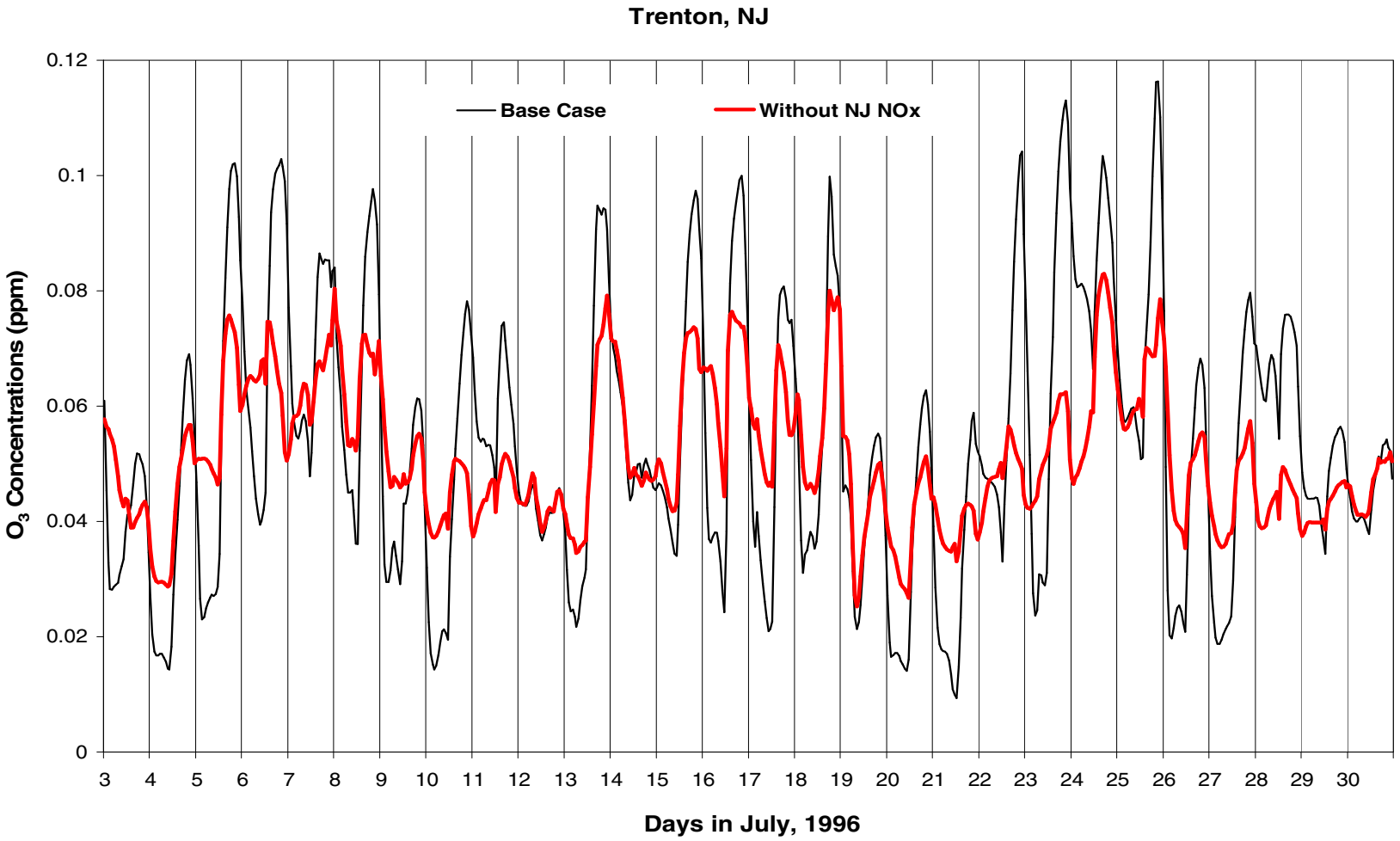

Figure S5. Time series of surface O_3 concentrations at Trenton, NJ during the July 1996 simulations. Baseline emissions with and without NJ NO_x emissions are plotted in black and red, respectively. Vertical lines indicate midnight on a given day.

SRC/RCP	AL	AZ	AR	CA	CO	CT	DE	FL	GA	ID	IL	IN	IA	KS	KY	LA	ME	MD	MA	MI	MN	MS	MO	MT	NE	NV	NH	NJ	NM	NY	NC	ND	OH	OK	OR	PA	RI	SC	SD	TN	TX	UT	VT	VA	WA	WV	WI	WY
AL	27.4	0.0	0.0	0.0	0.0	0.0	0.0	11.4	14.3	0.0	0.0	0.0	0.0	0.0	2.1	2.9	0.0	0.0	0.0	0.0	0.0	11.3	0.0	0.0	0.0	0.0	0.0	0.0	0.0	0.0	5.1	0.0	0.0	0.0	0.0	0.0	0.0	3.9	0.0	8.5	0.0	0.0	0.0	1.9	0.0	0.0	0.0	0.0
AZ	0.0	42.1	0.0	10.5	3.4	0.0	0.0	0.0	0.0	0.0	0.0	0.0	0.0	1.2	0.0	0.0	0.0	0.0	0.0	0.0	0.0	0.0	0.0	0.0	0.0	10.5	0.0	0.0	15.2	0.0	0.0	0.0	0.0	1.6	0.0	0.0	0.0	0.0	0.0	0.0	3.2	12.4	0.0	0.0	0.0	0.0	0.0	0.0
AR	3.0	0.0	12.7	0.0	0.0	0.0	0.0	0.0	1.8	0.0	3.9	1.6	0.0	1.2	4.9	6.8	0.0	0.0	0.0	0.0	0.0	11.8	9.8	0.0	0.0	0.0	0.0	0.0	0.0	0.0	1.6	0.0	0.0	5.5	0.0	0.0	0.0	1.2	0.0	12.7	3.9	0.0	0.0	1.0	0.0	0.0	0.0	0.0
CA	0.0	37.3	0.0	54.2	4.1	0.0	0.0	0.0	0.0	2.0	0.0	0.0	0.0	0.8	0.0	0.0	0.0	0.0	0.0	0.0	0.0	0.0	0.0	0.8	1.7	37.3	0.0	0.0	3.7	0.0	0.0	0.0	0.0	1.0	2.2	0.0	0.0	0.0	0.9	0.0	0.9	18.7	0.0	0.0	0.0	0.0	0.0	2.6
CO	0.0	2.2	0.0	0.0	24.3	0.0	0.0	0.0	0.0	0.0	0.0	0.0	0.0	8.8	0.0	0.0	0.0	0.0	0.0	0.0	0.0	0.0	0.0	0.0	9.4	0.0	0.0	0.0	5.4	0.0	0.0	0.0	0.0	4.5	0.0	0.0	0.0	0.0	1.1	0.0	2.4	3.6	0.0	0.0	0.0	0.0	0.0	10.7
CT	0.0	0.0	0.0	0.0	0.0	7.1	0.0	0.0	0.0	0.0	0.0	0.0	0.0	0.0	0.0	0.0	1.3	0.0	4.9	0.0	0.0	0.0	0.0	0.0	0.0	0.0	1.8	0.0	0.0	4.4	0.0	0.0	0.0	0.0	0.0	0.0	7.1	0.0	0.0	0.0	0.0	0.0	1.7	0.0	0.0	0.0	0.0	0.0
DE	0.0	0.0	0.0	0.0	0.0	0.0	13.7	0.0	0.0	0.0	0.0	0.0	0.0	0.0	0.0	0.0	0.0	4.7	0.0	0.0	0.0	0.0	0.0	0.0	0.0	0.0	0.0	13.7	0.0	1.0	0.0	0.0	0.0	0.0	0.0	3.7	0.0	0.0	0.0	0.0	0.0	0.0	0.0	1.0	0.0	0.0	0.0	0.0
FL	10.2	0.0	0.0	0.0	0.0	0.0	0.0	30.2	15.6	0.0	0.0	0.0	0.0	0.0	0.0	2.7	0.0	0.0	0.0	0.0	0.0	3.2	0.0	0.0	0.0	0.0	0.0	0.0	0.0	0.0	2.1	0.0	0.0	0.0	0.0	0.0	0.0	7.8	0.0	0.0	0.0	0.0	0.0	0.0	0.0	0.0	0.0	0.0
GA	11.5	0.0	0.0	0.0	0.0	0.0	0.0	5.7	25.5	0.0	0.0	0.0	0.0	0.0	1.6	0.0	0.0	0.0	0.0	0.0	0.0	0.0	0.0	0.0	0.0	0.0	0.0	0.0	0.0	0.0	7.1	0.0	0.0	0.0	0.0	0.0	0.0	17.4	0.0	10.6	0.0	0.0	0.0	1.9	0.0	0.0	0.0	0.0
ID	0.0	0.0	0.0	0.0	1.3	0.0	0.0	0.0	0.0	16.3	0.0	0.0	0.0	0.0	0.0	0.0	0.0	0.0	0.0	0.0	0.0	0.0	0.0	1.9	0.0	4.9	0.0	0.0	0.0	0.0	0.0	0.0	0.0	0.0	7.4	0.0	0.0	0.0	0.0	0.0	0.0	6.0	0.0	0.0	6.8	0.0	0.0	3.2
IL	2.0	0.0	4.0	0.0	0.0	0.0	0.0	0.0	1.9	0.0	18.4	12.3	9.7	0.0	12.2	0.0	0.0	2.1	0.0	8.5	1.4	2.6	18.4	0.0	1.0	0.0	0.0	0.9	0.0	2.0	1.9	0.0	3.6	0.0	0.0	2.2	0.0	1.5	0.0	6.2	0.0	0.0	0.0	2.4	0.0	2.5	8.5	0.0
IN	1.5	0.0	0.8	0.0	0.0	0.0	0.9	0.0	1.6	0.0	13.0	13.5	0.0	0.0	12.4	0.0	0.0	2.4	0.0	8.5	0.0	1.1	2.0	0.0	0.0	0.0	0.9	1.0	0.0	2.0	3.0	0.0	12.3	0.0	0.0	2.6	0.0	1.5	0.0	3.6	0.0	0.0	1.0	3.9	0.0	3.4	2.9	0.0
IA	0.0	0.0	1.1	0.0	0.0	0.0	0.0	0.0	0.0	0.0	8.2	1.8	9.0	3.2	1.0	0.0	0.0	0.0	0.0	1.3	4.2	0.8	6.5	0.0	8.2	0.0	0.0	0.0	0.0	0.0	0.0	1.0	1.0	1.0	0.0	0.8	0.0	0.0	4.9	1.0	0.0	0.0	0.0	0.0	0.0	0.0	6.2	0.0
KS	0.0	0.0	2.0	0.0	5.3	0.0	0.0	0.0	0.0	0.0	1.1	0.0	2.4	12.0	0.0	0.0	0.0	0.0	0.0	0.0	1.1	0.0	12.0	0.0	7.1	0.0	0.0	0.0	0.0	0.0	0.0	0.0	0.0	6.0	0.0	0.0	0.0	0.0	1.5	0.0	1.8	0.0	0.0	0.0	0.0	0.0	0.0	0.0
KY	2.0	0.0	2.8	0.0	0.0	0.0	1.0	0.0	2.5	0.0	10.0	12.8	0.0	0.0	13.1	0.0	0.0	2.8	0.0	0.9	0.0	1.6	8.0	0.0	0.0	0.0	0.0	0.9	0.0	1.5	4.6	0.0	12.4	0.0	0.0	3.5	0.0	2.5	0.0	8.3	0.0	0.0	0.0	8.3	0.0	12.0	0.0	0.0
LA	9.7	0.0	16.5	0.0	0.0	0.0	0.0	6.0	3.3	0.0	1.3	0.9	0.0	0.0	1.4	27.5	0.0	0.0	0.0	0.0	0.0	23.6	1.8	0.0	0.0	0.0	0.0	0.0	0.0	0.0	1.2	0.0	0.0	1.6	0.0	0.0	0.0	1.7	0.0	3.5	20.9	0.0	0.0	0.0	0.0	0.0	0.0	0.0
ME	0.0	0.0	0.0	0.0	0.0	0.0	0.0	0.0	0.0	0.0	0.0	0.0	0.0	0.0	0.0	0.0	3.2	0.0	0.0	0.0	0.0	0.0	0.0	0.0	0.0	0.0	1.0	0.0	0.0	0.0	0.0	0.0	0.0	0.0	0.0	0.0	0.0	0.0	0.0	0.0	0.0	0.0	0.0	0.0	0.0	0.0	0.0	0.0
MD	0.0	0.0	0.0	0.0	0.0	1.8	14.9	0.0	0.0	0.0	0.0	0.0	0.0	0.0	0.0	0.0	1.3	34.1	1.8	0.0	0.0	0.0	0.0	0.0	0.0	0.0	1.3	14.9	0.0	2.4	4.1	0.0	0.0	0.0	0.0	13.6	1.8	0.0	0.0	0.0	0.0	0.0	0.9	12.9	0.0	7.8	0.0	0.0
MA	0.0	0.0	0.0	0.0	0.0	3.1	0.0	0.0	0.0	0.0	0.0	0.0	0.0	0.0	0.0	0.0	5.3	0.0	8.9	0.0	0.0	0.0	0.0	0.0	0.0	0.0	4.3	0.0	0.0	1.2	0.0	0.0	0.0	0.0	0.0	0.0	2.7	0.0	0.0	0.0	0.0	0.0	3.0	0.0	0.0	0.0	0.0	0.0
MI	0.0	0.0	0.0	0.0	0.0	1.6	1.0	0.0	0.0	0.0	2.4	5.1	0.0	0.0	1.3	0.0	1.3	1.5	2.0	12.9	1.4	0.0	0.0	0.0	0.0	0.0	1.9	1.0	0.0	6.5	0.9	0.0	9.5	0.0	0.0	6.5	1.1	0.0	0.0	1.0	0.0	0.0	2.0	1.5	0.0	2.3	6.2	0.0
MN	0.0	0.0	0.0	0.0	0.0	0.0	0.0	0.0	0.0	0.0	2.7	1.6	7.8	1.7	0.0	0.0	0.0	0.0	0.0	3.8	11.6	0.0	2.0	0.0	2.4	0.0	0.0	0.0	0.0	0.0	0.0	5.5	1.0	0.0	0.0	0.0	0.0	0.0	5.2	0.0	0.0	0.0	0.0	0.0	0.0	0.0	11.6	0.0
MS	12.1	0.0	6.3	0.0	0.0	0.0	0.0	4.7	2.2	0.0	1.2	0.0	0.0	0.0	1.6	11.5	0.0	0.0	0.0	0.0	0.0	14.2	2.2	0.0	0.0	0.0	0.0	0.0	0.0	0.0	1.5	0.0	0.0	0.0	0.0	0.0	0.0	1.4	0.0	8.6	0.0	0.0	0.0	0.0	0.0	0.0	0.0	0.0
MO	1.6	0.0	7.3	0.0	0.0	0.0	0.0	0.0	1.2	0.0	13.3	5.0	5.7	10.7	10.4	1.4	0.0	1.0	0.0	1.0	1.3	2.5	13.3	0.0	5.6	0.0	0.0	0.0	0.0	0.0	1.0	0.0	1.7	7.4	0.0	1.0	0.0	0.8	1.1	10.4	0.9	0.0	0.0	1.3	0.0	1.2	1.2	0.0
MT	0.0	0.0	0.0	0.0	0.0	0.0	0.0	0.0	0.0	1.5	0.0	0.0	0.0	0.0	0.0	0.0	0.0	0.0	0.0	0.0	0.0	0.0	0.0	10.2	1.6	0.0	0.0	0.0	0.0	0.0	0.0	2.8	0.0	0.0	0.0	0.0	0.0	0.0	2.8	0.0	0.0	0.0	0.0	0.0	0.0	0.0	0.0	6.6
NE	0.0	0.0	0.8	0.0	4.9	0.0	0.0	0.0	0.0	0.0	0.0	0.0	8.2	6.5	0.0	0.0	0.0	0.0	0.0	0.0	2.1	0.0	7.6	0.0	9.4	0.0	0.0	0.0	0.0	0.0	0.0	1.2	0.0	0.9	0.0	0.0	0.0	0.0	5.4	0.0	0.0	0.0	0.0	0.0	0.0	0.0	0.0	2.7
NV	0.0	9.5	0.0	7.2	0.0	0.0	0.0	0.0	0.0	0.0	0.0	0.0	0.0	0.0	0.0	0.0	0.0	0.0	0.0	0.0	0.0	0.0	0.0	0.0	0.0	18.8	0.0	0.0	0.0	0.0	0.0	0.0	0.0	0.0	0.0	0.0	0.0	0.0	0.0	0.0	0.0	7.2	0.0	0.0	0.0	0.0	0.0	0.0
NH	0.0	0.0	0.0	0.0	0.0	0.0	0.0	0.0	0.0	0.0	0.0	0.0	0.0	0.0	0.0	0.0	3.4	0.0	3.4	0.0	0.0	0.0	0.0	0.0	0.0	0.0	3.4	0.0	0.0	0.0	0.0	0.0	0.0	0.0	0.0	0.0	0.0	0.0	0.0	0.0	0.0	0.0	1.3	0.0	0.0	0.0	0.0	0.0
NJ	0.0	0.0	0.0	0.0	0.0	9.7	15.3	0.0	0.0	0.0	0.0	0.0	0.0	0.0	0.0	0.0	2.8	4.5	6.0	0.0	0.0	0.0	0.0	0.0	0.0	0.0	3.1	28.1	0.0	12.6	1.0	0.0	0.0	0.0	0.0	16.7	6.7	0.0	0.0	0.0	0.0	0.0	3.1	2.0	0.0	0.0	0.0	0.0
NM	0.0	8.6	0.0	0.0	16.3	0.0	0.0	0.0	0.0	0.0	0.0	0.0	0.0	3.2	0.0	0.0	0.0	0.0	0.0	0.0	0.0	0.0	0.0	0.0	0.8	0.0	0.0	0.0	16.9	0.0	0.0	0.0	0.0	4.6	0.0	0.0	0.0	0.0	0.0	0.0	7.5	6.6	0.0	0.0	0.0	0.0	0.0	0.0
NY	0.0	0.0	0.0	0.0	0.0	12.5	0.0	0.0	0.0	0.0	0.0	0.0	0.0	0.0	0.0	0.0	3.7	0.0	7.4	0.0	0.0	0.0	0.0	0.0	0.0	0.0	4.7	5.4	0.0	12.9	0.0	0.0	0.0	0.0	0.0	4.0	9.7	0.0	0.0	0.0	0.0	0.0	6.7	0.0	0.0	0.0	0.0	0.0
NC	0.9	0.0	0.0	0.0	0.0	1.2	1.9	0.0	2.4	0.0	0.0	0.0	0.0	0.0	1.1	0.0	0.0	3.1	1.4	0.0	0.0	0.0	0.0	0.0	0.0	0.0	0.0	1.8	0.0	1.5	18.7	0.0	0.0	0.0	0.0	0.0	1.3	11.5	0.0	3.3	0.0	0.0	0.0	14.4	0.0	1.7	0.0	0.0
ND	0.0	0.0	0.0	0.0	0.0	0.0	0.0	0.0	0.0	0.0	0.0	0.0	1.1	0.0	0.0	0.0	0.0	0.0	0.0	0.0	4.2	0.0	0.0	2.3	1.5	0.0	0.0	0.0	0.0	0.0	0.0	7.1	0.0	0.0	0.0	0.0	0.0	0.0	4.5	0.0	0.0	0.0	0.0	0.0	0.0	0.0	0.0	0.0
OH	0.0	0.0	0.0	0.0	0.0	2.2	2.5	0.0	0.0	0.0	0.0	7.2	0.0	0.0	11.1	0.0	1.1	9.0	2.0	6.3	0.0	0.0	0.0	0.0	0.0	0.0	1.6	3.0	0.0	6.1	2.6	0.0	17.5	0.0	0.0	14.4	1.6	1.2	0.0	2.2	0.0	0.0	1.7	7.3	0.0	17.5	0.0	0.0
OK	1.1	0.0	9.2	0.0	4.3	0.0	0.0	0.0	0.0	0.0	1.2	0.0	0.9	11.9	1.1	0.9	0.0	0.0	0.0	0.0	0.0	1.3	9.2	0.0	2.2	0.0	0.0	0.0	1.4	0.0	0.0	0.0	0.0	18.8	0.0	0.0	0.0	0.0	0.0	1.1	6.6	0.0	0.0	0.0	0.0	0.0	0.0	0.0
OR	0.0	0.0	0.0	12.4	0.0	0.0	0.0	0.0	0.0	7.5	0.0	0.0	0.0	0.0	0.0	0.0	0.0	0.0	0.0	0.0	0.0	0.0	0.0	1.6	0.0	3.5	0.0	0.0	0.0	0.0	0.0	0.0	0.0	0.0	16.3	0.0	0.0	0.0	0.0	0.0	0.0	1.4	0.0	0.0	12.9	0.0	0.0	0.8
PA	0.0	0.0	0.0	0.0	0.0	5.8	10.7	0.0	0.0	0.0	0.0	0.0	0.0	0.0	0.0	0.0	2.1	10.7	4.1	0.0	0.0	0.0	0.0	0.0	0.0	0.0	2.8	18.5	0.0	13.7	2.8	0.0	2.6	0.0	0.0	18.5	4.1	0.0	0.0	0.0	0.0	0.0	3.3	5.8	0.0	5.8	0.0	0.0
RI	0.0	0.0	0.0	0.0	0.0	5.0	0.0	0.0	0.0	0.0	0.0	0.0	0.0	0.0	0.0	0.0	1.2	0.0	2.8	0.0	0.0	0.0	0.0	0.0	0.0	0.0	1.2	0.0	0.0	0.0	0.0	0.0	0.0	0.0	0.0	0.0	5.0	0.0	0.0	0.0	0.0	0.0	0.0	0.0	0.0	0.0	0.0	0.0
SC	0.0	0.0	0.0	0.0	0.0	0.0	0.0	0.0	8.2	0.0	0.0	0.0	0.0	0.0	0.0	0.0	0.0	0.8	0.0	0.0	0.0	0.0	0.0	0.0	0.0	0.0	0.0	0.8	0.0	0.0	15.0	0.0	0.0	0.0	0.0	0.0	0.0	15.0	0.0	0.0	0.0	0.0	0.0	1.3	0.0	0.0	0.0	0.0
SD	0.0	0.0	0.0	0.0	0.0	0.0	0.0	0.0	0.0	0.0	0.0	0.0	4.6	0.0	0.0	0.0	0.0	0.0	0.0	0.0	4.6	0.0	0.0	1.3	4.3	0.0	0.0	0.0	0.0	0.0	0.0	2.2	0.0	0.0	0.0	0.0	0.0	0.0	4.6	0.0	0.0	0.0	0.0	0.0	0.0	0.0	0.0	1.6
TN	7.0	0.0	13.1	0.0	0.0	0.0	0.0	0.0	11.1	0.0	5.7	3.2	0.0	0.0	10.9	1.3	0.0	1.1	0.0	0.0	0.0	10.7	9.5	0.0	0.0	0.0	0.0	0.0	0.0	0.0	11.3	0.0	2.3	0.0	0.0	0.0	0.0	3.4	0.0	14.7	0.0	0.0	0.0	9.3	0.0	4.2	0.0	0.0
TX	3.1	1.3	21.6	0.0	4.7	0.0	0.0	1.6	1.9	0.0	2.9	1.7	1.3	8.8	3.3	24.1	0.0	0.0	0.0	0.0	0.0	6.6	6.7	0.0	1.8	0.0	0.0	0.0	13.3	0.0	1.4	0.0	0.0	23.2	0.0	0.0	0.0	1.4	0.0	6.0	34.1	0.0	0.0	1.0	0.0	0.0	0.0	0.0
UT	0.0	11.7	0.0	0.0	7.3	0.0	0.0	0.0	0.0	7.9	0.0	0.0	0.0	0.0	0.0	0.0	0.0	0.0	0.0	0.0	0.0	0.0	0.0	0.0	0.9	1.7	0.0	0.0	2.8	0.0	0.0	0.0	0.0	0.0	0.0	0.0	0.0	0.0	0.0	0.0	0.0	38.7	0.0	0.0	0.0	0.0	0.0	5.2
VT	0.0	0.0	0.0	0.0	0.0	0.0	0.0	0.0	0.0	0.0	0.0	0.0	0.0	0.0	0.0	0.0	0.9	0.0	0.0	0.0	0.0	0.0	0.0	0.0	0.0	0.0	1.3	0.0	0.0	0.8	0.0	0.0	0.0	0.0	0.0	0.0	0.0	0.0	0.0	0.0	0.0	1.3	0.0	0.0	0.0	0.0	0.0	0.0
VA	0.0	0.0	0.0	0.0	0.0	2.1	7.1	0.0	0.0	0.0	0.0	0.0	0.0	0.0	3.5	0.0	1.0	20.8	2.2	0.0	0.0	0.0	0.0	0.0	0.0	0.0	1.0	5.2	0.0	2.4	13.3	0.0	0.0	0.0	0.0	4.8	2.1	1.3	0.0	5.2	0.0	0.0	0.0	22.2	0.0	7.9	0.0	0.0
WA	0.0	0.0	0.0	4.1	0.0	0.0	0.0	0.0	0.0	11.0	0.0	0.0	0.0	0.0	0.0	0.0	0.0	0.0	0.0	0.0	0.0	0.0	0.0	4.3	0.0	2.4	0.0	0.0	0.0	0.0	0.0	0.0	0.0	0.0	21.3	0.0	0.0	0.0	0.0	0.0	0.0	1.7	0.0	0.0	23.4	0.0	0.0	1.3
WV	0.0	0.0	0.0	0.0	0.0	0.0	0.9	0.0	0.0	0.0	0.0	0.0	0.0	0.0	1.5	0.0	0.0	5.5	0.0	0.0	0.0	0.0	0.0	0.0	0.0	0.0	0.0	0.9	0.0	0.0	1.1	0.0	3.6	0.0	0.0	4.8	0.0	0.0	0.0	0.0	0.0	0.0	0.0	4.9	0.0	5.7	0.0	0.0
WI	0.0	0.0	0.0	0.0	0.0	0.0	0.0	0.0	0.0	0.0	9.5	3.6	5.3	0.0	0.0	0.0	0.0	0.0	0.0	8.4	5.8	0.0	1.1	0.0	0.0	0.0	0.0	0.0	0.0	1.5	0.0	1.0	1.4	0.0	0.0	1.3	0.0	0.0	0.9	0.0	0.0	0.0	0.0	0.0	0.0	0.9	10.9	0.0
WY	0.0	0.0	0.0	0.0	9.6	0.0	0.0	0.0	0.0	1.2	0.0	0.0	0.0	1.7	0.0	0.0	0.0	0.0	0.0	0.0	0.0	0.0	0.0	4.1	9.6	0.0	0.0	0.0	0.0	0.0	0.0	1.1	0.0	0.0	0.0	0.0	0.0	0.0	4.2	0.0	0.0	4.4	0.0	0.0	0.0	0.0	0.0	12.3

Table S1. Maximum contribution to monthly mean peak 8-hour O_3 concentrations within a single grid cell over each receptor state resulting from a source state's NO_x emissions during July 1996.